Nonautonomous systems with transversal homoclinic structures under discretization

Alina Girod **Thorsten Hüls**

Abstract We consider homoclinic orbits in continuous time nonautonomous dynamical systems. Unlike the autonomous case, stable and unstable fiber bundles that generalize stable and unstable manifolds, typically intersect transversally in isolated points. In the first part, we establish persistence and error estimates for one–step discretizations of transversal homoclinic orbits. Secondly, we extend an algorithm by England, Krauskopf, Osinga to nonautonomous systems and illustrate transversally intersecting fibers along homoclinic orbits for three examples. The first one is constructed artificially in order to study numerical errors, while the second one is a periodically forced model that reveals the influence of underlying autonomous dynamics. The third example originates from mathematical biology.
Keywords: Nonautonomous dynamical systems, homoclinic orbits, fiber bundles, discretization effects, approximation theory, exponential dichotomy.
AMS Subject Classification: 70K44, 55R10, 37B55, 34C37

1 Introduction

Homoclinic structures in autonomous ODEs are characterized by the celebrated Smale–Šil'nikov–Birkhoff–Theorem, cf. [27, 28]. It turns out that they are a source of rich and even chaotic dynamics. This explains the importance of extensive studies for detecting these structures. Techniques for computing them numerically are introduced, for example, in [2, 8].

For autonomous ODEs with a homoclinic orbit w.r.t. an equilibrium, the corresponding stable and unstable manifolds [12] have the whole homoclinic

Supported by CRC 701 'Spectral Structures and Topological Methods in Mathematics'.

Department of Mathematics, Bielefeld University
POB 100131, 33501 Bielefeld, Germany
E-mail: agirod@uni-bielefeld.de huels@math.uni-bielefeld.de

orbit in common. However, Fiedler and Scheurle [7] showed that these manifolds generically split under time discretization (with an exponentially small splitting angle when the nonlinearities are analytic). More specifically Beyn and Zou proved in [30] that a one–step discretization of a parameter dependent ODE results in a discrete time system with a closed loop of homoclinic orbits. At a turning point of this loop, stable and unstable manifolds touch tangentially, while their intersection is transversal, otherwise, see Figure 1.1.

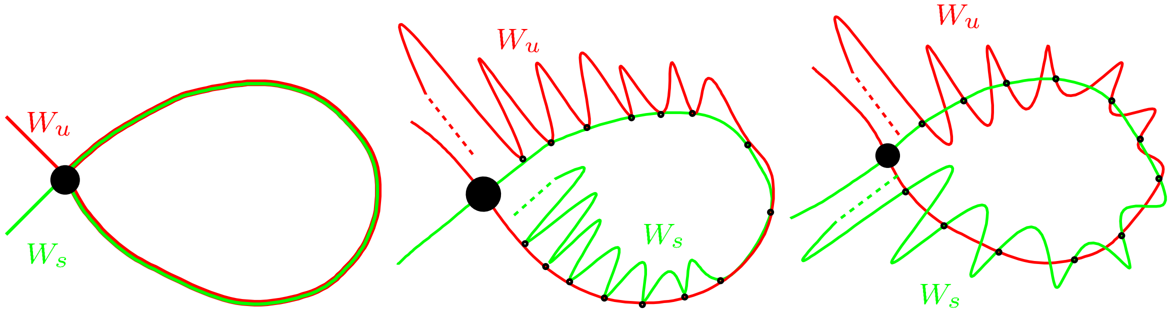

Fig. 1.1 Homoclinic orbits in autonomous systems: Manifolds before (left) and after discretization by a one–step method; tangential case (center) and transversal intersections (right).

Realistic models, for example, from mathematical biology are nonautonomous. This may be caused by seasonal fluctuations of the environment that cannot be handled adequately in autonomous models. Note that in a nonautonomous setup, one can hardly expect to find time independent fixed points. The only meaningful replacement of a fixed point is a bounded trajectory, see [21], and the corresponding stable and unstable manifolds also depend on time and are called stable and unstable fiber bundles, see e.g. [1].

If stable and unstable fiber bundles of a nonautonomous ODE intersect, then the point of intersection is in general isolated. It is important to mention that contrary to the autonomous case, stable and unstable fiber bundles typically do not have the whole orbit in common and consequently, the autonomous setup is not a special case of the nonautonomous situation. Depending on the system, one can expect to find a finite or a countable set of intersecting points between these fibers. In the latter case, Lerman and Šil'nikov [22] proved that the corresponding homoclinic orbits allow a symbolic coding and in this way create chaotic dynamics.

The aim of this paper is a deeper understanding of the interplay between continuous time and discrete time dynamics in a nonautonomous context. As a prototype, we analyze the fate of homoclinic orbits in nonautonomous ODEs under discretizations. It turns out that these orbits as well as corresponding transversal intersections of stable and unstable fiber bundles persist under one–step methods, see Theorem 4.2 and Figure 1.2.

As a first application, we construct a nonautonomous ODE having an explicitly known homoclinic orbit. Homoclinic orbits are computed numerically

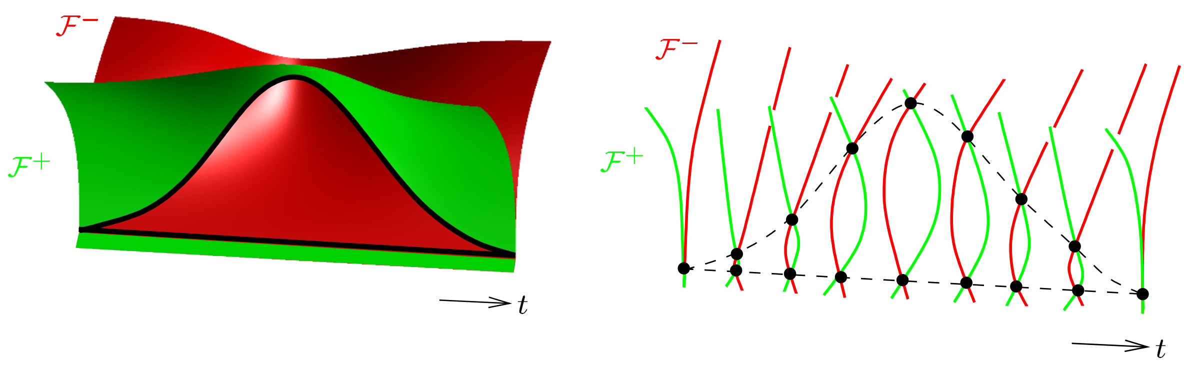

Fig. 1.2 Homoclinic orbits in nonautonomous systems: Fiber bundles before (left) and after (right) discretization by a one–step method.

using a one–step scheme in Section 5, with a subsequent discussion of approximation errors.

For illustrating transversally intersecting fiber bundles in discrete time, adequate tools for their numerical approximation are needed. Note that the resulting maps are noninvertible in general. We tackle this problem in Section 5.2 by introducing a nonautonomous generalization of an algorithm by England, Krauskopf and Osinga, see [6]. It computes one–dimensional stable fiber bundles in a two–dimensional system. The algorithm starts with a linear approximation of a stable fiber that can be expressed by the subspaces of an exponential dichotomy, see [15] for an approach that allows their computation. We then search for pre–images that lie in the previous fiber and avoid in this way the use of the inverse mapping. Continuing this idea, the approximate fiber bundles grow.

Using this algorithm, we compute fiber bundles for a discretization of our first ODE and of a periodically forced version.

Finally, we apply our techniques to a two–dimensional nonautonomous model from mathematical biology, see [26], that exhibits transversally intersecting stable and unstable fiber bundles and thus, homoclinic orbits.

2 Homoclinic orbits in continuous time

We start by introducing basic assumptions and the notion of a transversal homoclinic orbit for a nonautonomous system in continuous time.

Consider the nonautonomous differential equation

$$\dot{x} = f(x,t) \quad \text{for } x \in \mathbb{R}^k,\ t \in \mathbb{R} \tag{2.1}$$

and denote by $\varphi(x,t,s)$ its solution operator transferring the solution from time s to time t. For this system, we impose the following assumptions:

(A1) $f \in \mathcal{C}^1(\mathbb{R}^k \times \mathbb{R}, \mathbb{R})$ satisfies conditions, assuring existence and uniqueness of global solutions as well as the following estimates for the solution operator.

For any compact set $\mathcal{K} \subset \mathbb{R}^k$ there exist constants $C_1(\mathcal{K}), h_1(\mathcal{K}) > 0$ such that the inequality

$$\|\varphi_x(x,t,s)\| \le C_1(\mathcal{K})$$

holds for all $x \in \mathcal{K}$ and $|t-s| \le h_1(\mathcal{K})$. For $n \in \mathbb{Z}$ let $\varphi_n(x,h) := \varphi(x,(n+1)h, nh)$ be $\mathcal{C}^d$ smooth w.r.t. h, $d \ge 1$. Mixed derivatives $(\varphi_n)_{x,h}^{(1,\ell)}$, $\ell \in \{0,\dots,d\}$ exist and satisfy the uniform Lipschitz condition

$$\left\|(\varphi_n)_{x,h}^{(1,d)}(x,\mu_1) - (\varphi_n)_{x,h}^{(1,d)}(x,\mu_2)\right\| \le C_1(\mathcal{K})\,\|\mu_1-\mu_2\|$$

for all $x \in \mathcal{K}$, $0 \le \mu_1, \mu_2 \le h_1(\mathcal{K})$ and $n \in \mathbb{Z}$.
Further, let $\left\|(\varphi_n)_{x,h}^{(r,1)}(x,h)\right\| \le C_1(\mathcal{K})$ for all $n \in \mathbb{Z}$, $r \in \{0,1\}$, $x \in \mathcal{K}$ and $0 \le h \le h_1(\mathcal{K})$.

Here, upper and lower indicies denote partial derivatives

$$(\varphi_n)_{x,h}^{(i,j)}(x,h) := \frac{\partial^i}{\partial x^i}\frac{\partial^j}{\partial h^j}\varphi_n(x,h).$$

(A2) $0 \in \mathbb{R}^k$ satisfies $f(0,t) = 0$ for all $t \in \mathbb{R}$.
(A3) 0 is **hyperbolic**, i.e. the variational equation

$$\dot{x} = f_x(0,\cdot)x$$

has an exponential dichotomy on $\mathbb{R}$, cf. Def. A.1. Denote the corresponding dichotomy data by $(K, \beta, P_t^{s,u})$.

The Banach space of bounded functions is defined as

$$X^i = \left\{u(\cdot) \in C^1(\mathbb{R},\mathbb{R}^k) : \|u\|_i = \sum_{j=0}^{i} \sup_{t\in\mathbb{R}} \left\|u^{(j)}(t)\right\|_\infty < \infty\right\}.$$

If (2.1) possesses a (hyperbolic) bounded solution $\xi(\cdot) \in X^0$, then the transformed system

$$\dot{y} = g(y,t), \quad g(y,t) := f(y+\xi(t),t) - f(\xi(t),t)$$

has 0 as a t–independent (hyperbolic) equilibrium. Thus without loss of generality **(A2)** is fulfilled. Note that **(A1)** is invariant under this transformation.

We introduce the notion of homoclinic orbits in nonautonomous systems:

Definition 2.1 Two **bounded trajectories** $x(\cdot)$ and $y(\cdot)$ of (2.1) are **homoclinic** toward each other if

$$\lim_{\substack{t\to\pm\infty,\\ t\in\mathbb{R}}} \|x(t)-y(t)\| = 0. \tag{2.2}$$

Note that homoclinic orbits in discrete time systems are defined similarly but t is restricted to $\mathbb{Z}$, see [16].

Assuming **(A3)**, the trajectory $y(t) = 0$ for all t is trivial and (2.2) has the form $\lim_{t\to\pm\infty} x(t) = 0$ if $x(\cdot)$ is homoclinic w.r.t. the equilibrium 0. Unless stated otherwise, homoclinic always means homoclinic w.r.t. the equilibrium 0. We further assume existence and transversality of this homoclinic orbit.

(A4) A nontrivial homoclinic orbit $\bar{x}(\cdot)$ of (2.1) exists.
(A5) The homoclinic orbit $\bar{x}(\cdot)$ is **transversal** in the following sense:

$$\dot{u}(t) = f_x(\bar{x}(t), t)u(t),\ t \in \mathbb{R} \text{ with } u(\cdot) \in X^1 \Leftrightarrow u(\cdot) = 0.$$

Geometrically, transversality means that stable and unstable fiber bundles intersect transversally along the homoclinic orbit. The definition of invariant fiber bundles in continuous time can be found in [25]. Note that invariant fiber bundles in discrete time systems are defined similarly, see [1]. They are the nonautonomous equivalent of the hyperbolic manifolds in the autonomous case.

Definition 2.2 Stable and unstable global fiber bundles of the fixed point 0 of equation (2.1) are defined as

$$\mathcal{F}^\pm := \{(t,x) \in \mathbb{R} \times \mathbb{R}^k : \lim_{s\to\pm\infty} \varphi(x,s,t) = 0\}$$

and **global** t**–fibers** are $\mathcal{F}^\pm(t) := \{x \in \mathbb{R}^k : (t,x) \in \mathcal{F}^\pm\}$.

Local fiber bundles w.r.t. a neighborhood $U \subset \mathbb{R}^k$ of 0 are defined as

$$\mathcal{F}_U^+ := \{(t,x) \in \mathcal{F}^+ : \varphi(x,s,t) \in U \quad \forall s \geq t\},$$
$$\mathcal{F}_U^- := \{(t,x) \in \mathcal{F}^- : \varphi(x,s,t) \in U \quad \forall s \leq t\}$$

and **local** t**–fibers** are $\mathcal{F}_U^\pm(t) := \{x \in \mathbb{R}^k : (t,x) \in \mathcal{F}_U^\pm\}$.

Alternative characterizations of transversality are summarized in

Theorem 2.1 *Assume* **(A1)**–**(A4)**, *then the following statements are equivalent*

(a$_c$) *The homoclinic orbit $\bar{x}(\cdot)$ is transversal in the sense of* **(A5)**.
(b$_c$) *The variational equation*

$$\dot{u} = f_x(\bar{x}(\cdot), \cdot)u \tag{2.3}$$

has an exponential dichotomy on $\mathbb{R}$.
(c$_c$) *The linear operator*

$$L(\bar{x}) : X^1 \to X^0,\ L(\bar{x})u(\cdot) := \dot{u}(\cdot) - f_x(\bar{x}(\cdot), \cdot)u(\cdot)$$

is a homeomorphism.
(d$_c$) *The tangent spaces $T_{\bar{x}(0)}\mathcal{F}^\pm(0)$ of the fibers $\mathcal{F}^\pm(0)$ at the point $\bar{x}(0)$ satisfy*

$$T_{\bar{x}(0)}\mathcal{F}^-(0) \oplus T_{\bar{x}(0)}\mathcal{F}^+(0) = \mathbb{R}^k.$$

Proof $(\mathrm{a_c})\Rightarrow(\mathrm{b_c})$: Since $\bar{x}$ is a homoclinic orbit w.r.t. the hyperbolic equilibrium 0, the Roughness–Theorem [5, Prop.1] applies and gives an exponential dichotomy of (2.3) that one can extend to $\mathbb{R}^+$ and $\mathbb{R}^-$. By assuming $(\mathrm{a_c})$, a nontrivial bounded solution cannot exist. Using [23, Prop. 2.1] half sided dichotomies can be combined into a dichotomy on $\mathbb{R}$.

$(\mathrm{b_c})\Rightarrow(\mathrm{c_c})$: Assuming $(\mathrm{b_c})$ $\mathcal{N}(L(\bar{x})) = \{0 \in X^1\}$ directly follows. On the other hand, we obtain for each $r \in X^0$ – using Green's function – a unique bounded solution in X^1 of the inhomogeneous equation

$$\dot{u} = f_x(\bar{x}(\cdot), \cdot)u + r(\cdot).$$

Thus $L(\bar{x})$ is injective and surjective.

$(\mathrm{c_c})\Rightarrow(\mathrm{a_c})$: The claim immediately follows, since $L(\bar{x})$ is a homeomorphism.

$(\mathrm{a_c})\Leftrightarrow(\mathrm{d_c})$: For a proof we refer to the end of Section 3 where we introduce the discrete equivalent of these statements.

□

Several of the following results hold true for bounded trajectories that need not to be homoclinic. In this case, we assume

(A6) Let $\bar{y}(\cdot)$ be a hyperbolic bounded trajectory of (2.1). Denote by $(\bar{K}, \bar{\beta}, \bar{Q}_t^{s,u})$ the dichotomy data of the corresponding variational equation

$$\dot{u} = f_x(\bar{y}(\cdot), \cdot)u$$

and let $S^{\bar{y}}(s,t)$ be its solution operator.

3 Discretization by the h–flow

In this section, we discretize the differential equation (2.1), using the h–flow. From a numerical point of view, this ansatz is of no practical relevance. It is introduced for deriving error estimates of one–step methods in Section 4.

We consider the h–flow

$$\varphi_n(x,h) := \varphi(x,(n+1)h,nh) \tag{3.1}$$

and note that the resulting dynamical system is invertible. A $\varphi_{\mathbb{Z}}(\cdot,h)$–orbit is a zero of the operator

$$\Gamma : S_{\mathbb{Z}} \times \mathbb{R} \to S_{\mathbb{Z}},\ (x_{\mathbb{Z}}, h) \mapsto (x_{n+1} - \varphi_n(x_n,h))_{n\in\mathbb{Z}}$$

that operates on the Banach space of bounded sequences

$$S_{\mathbb{Z}} := \left\{ x_{\mathbb{Z}} = (x_n)_{n\in\mathbb{Z}} : x_n \in \mathbb{R}^k, \|x_{\mathbb{Z}}\| := \sup_{n\in\mathbb{Z}} \|x_n\| < \infty \right\}.$$

Assuming **(A6)**, the discretized orbit

$$\bar{y}_{\mathbb{Z}}(h) := (\bar{y}_n(h))_{n\in\mathbb{Z}} := (\bar{y}(nh))_{n\in\mathbb{Z}}$$

is bounded and a zero of Γ.

Further, we look at the corresponding variational equation that we obtain by differentiating Γ w.r.t. the first component

$$\Gamma_{x_{\mathbb{Z}}}(\bar{y}_{\mathbb{Z}}(h),h) : S_{\mathbb{Z}} \to S_{\mathbb{Z}},\ u_{\mathbb{Z}} \mapsto (u_{n+1} - (\varphi_n)_x(\bar{y}_n(h),h)u_n)_{n\in\mathbb{Z}}.$$

Transversality of homoclinic orbits $x_{\mathbb{Z}}(h)$ in discrete time systems is characterized by one of the equivalent properties given in Theorem 3.1, see Theorem 2.1 for the continuous time case and note that all results applied in the proof have a discrete time counterpart. We particularly refer to [13, Lemma 3.7] for the equivalence of (a$_\Delta$) and (d$_\Delta$).

Theorem 3.1 *Assume* **(A1)**–**(A4)** *and let* $h > 0$. *Then* $\bar{x}_{\mathbb{Z}}(h)$ *is a homoclinic orbit of* (3.1). *Furthermore, the following statements are equivalent:*

(a$_\Delta$) $u_{n+1} = (\varphi_n)_x(\bar{x}_n(h),h)u_n, \quad u_{\mathbb{Z}} \in S_{\mathbb{Z}} \quad \Leftrightarrow \quad u_{\mathbb{Z}} = 0.$

(b$_\Delta$) *The variational equation*

$$u_{n+1} = (\varphi_n)_x(\bar{x}_n(h),h)u_n, \quad n \in \mathbb{Z}$$

has an exponential dichotomy on $\mathbb{Z}$.

(c$_\Delta$) $\Gamma_{x_{\mathbb{Z}}}(\bar{x}_{\mathbb{Z}},h)$ *is a homeomorphism.*

(d$_\Delta$) *The tangent spaces* $T_{\bar{x}_0}\mathcal{F}_h^{\pm}(0)$ *of the global stable and unstable* 0*–fibers* $\mathcal{F}_h^{\pm}(0)$ *of the h–flow* $x_{n+1} = \varphi_n(x_n,h)$ *satisfy*

$$T_{\bar{x}_0}\mathcal{F}_h^{-}(0) \oplus T_{\bar{x}_0}\mathcal{F}_h^{+}(0) = \mathbb{R}^k.$$

We show that the stable and unstable fiber bundles of the continuous system coincide with those of the system defined by the h–flow for h sufficiently small.

Lemma 3.1 *Assume* **(A1)** *and* **(A2)**. *Then there exists a constant* $\hat{h} > 0$ *such that*

$$\mathcal{F}^{\pm}(0) = \mathcal{F}_h^{\pm}(0)$$

holds for all $0 < h < \hat{h}$.

Proof $\mathcal{F}^{\pm}(0) \subset \mathcal{F}_h^{\pm}(0)$ is trivial. For proving the other inclusion let $x_0 \in \mathcal{F}_h^{\pm}(0)$. For every $t \in \mathbb{R}$ we find an $n \in \mathbb{Z}$ such that $nh \le t \le (n+1)h$ holds. With **(A1)**, **(A2)** and the mean value theorem we get

$$\begin{aligned}
&\sup_{nh\le t\le(n+1)h} \|\varphi(x_0,t,0)\| \\
=&\sup_{nh\le t\le(n+1)h} \|\varphi(\varphi(x_0,nh,0),t,nh) - \varphi(0,t,nh)\| \\
=&\sup_{nh\le t\le(n+1)h} \left\| \int_0^1 \varphi_x(s\varphi(x_0,nh,0),t,nh)\mathrm{d}s\varphi(x_0,nh,0)\right\| \\
\le& C_1\|\varphi(x_0,nh,0)\|.
\end{aligned} \tag{3.2}$$

From $x_0 \in \mathcal{F}_h^{\pm}(0)$ it follows that $\lim_{n\to\pm\infty} \varphi(x_0,nh,0) = 0$ holds. With (3.2) we get $\lim_{t\to\pm\infty} \varphi(x_0,t,0) = 0$ and consequently $x_0 \in \mathcal{F}^{\pm}(0)$. $\square$

Also hyperbolicity as well as transversality of a trajectory in continuous time carries over to the discrete trajectory generated by the h–flow.

Lemma 3.2 (a) *Assume* **(A1)** *and* **(A6)**, *then* $\bar{y}_{\mathbb{Z}}(h)$ *is a hyperbolic bounded trajectory of* $\varphi_n(\cdot, h)$ *for all* $h > 0$.
(b) *Assume* **(A1)**–**(A4)**, *then the following statements are equivalent:*
(b$_1$) *The continuous time orbit* $\bar{x}(\cdot)$ *is transversal in the sense of* **(A5)**.
(b$_2$) *There exists an* $\hat{h} > 0$ *such that* $\bar{x}_{\mathbb{Z}}(h)$ *is a transversal homoclinic orbit of the h–flow* $\varphi_n(\cdot, h)$ *for all step sizes* $0 < h \leq \hat{h}$.

Proof Let $h > 0$ and assume **(A1)** as well as **(A6)**. Denote by Φ the solution operator of the variational equation

$$u_{n+1} = (\varphi_n)_x(\bar{y}_n(h), h)u_n, \quad n \in \mathbb{Z} \tag{3.3}$$

and observe that

$$\Phi(n, m) = S^{\bar{y}}(nh, mh), \quad n, m \in \mathbb{Z}.$$

Using the continuous time dichotomy data from **(A6)**, we define

$$Q_n^{s,u}(h) := \bar{Q}_{hn}^{s,u}, \ n \in \mathbb{Z}$$

and immediately obtain that (3.3) has an exponential dichotomy on $\mathbb{Z}$ with data $(\bar{K}, h\bar{\beta}, Q_n^{s,u}(h))$. This completes the proof of (a).

For proving (b) assume **(A1)**–**(A4)**. If (b$_1$) holds true, then Theorem 2.1 guarantees that (2.3) has an exponential dichotomy on $\mathbb{R}$. An application of (a) combined with the observation that the h–flow preserves homoclinic structures proves (b$_2$).

To show the implication "(b$_2$)$\Rightarrow$(b$_1$)", we assume that (b$_1$) is not satisfied, i.e. the orbit $\bar{x}(\cdot)$ is not transversal. Then a nontrivial bounded solution $u(\cdot)$ of (2.3) exists. As a consequence, we find an $\tilde{h} > 0$ such that $u_{\mathbb{Z}}(h) = (u(nh))_{n\in\mathbb{Z}} \neq 0$ for all $0 < h \leq \tilde{h}$ and $u_{n+1}(h) = S^{\bar{x}}((n+1)h, nh)u_n(h)$ holds for all $n \in \mathbb{Z}$, where $S^{\bar{x}}(s, t)$ is the solution operator of (2.3). Applying the identity

$$S^{\bar{x}}((n+1)h, nh) = (\varphi_n)_x(\bar{x}_n(h), h)$$

for all $n \in \mathbb{Z}$ we obtain

$$u_{n+1}(h) = (\varphi_n)_x(\bar{x}_n, h)u_n(h), \quad n \in \mathbb{Z}.$$

Since $u_{\mathbb{Z}}(h) \neq 0$ for all $h \leq \tilde{h}$ Theorem 3.1 (a$_\Delta$) applies and thus $\bar{x}_{\mathbb{Z}}(h)$ is not transversal for all $h \leq \tilde{h}$. This violates condition (b$_2$). □

Combining these results, we prove the remaining statements of Theorem 2.1.

Proof of Theorem 2.1, "(a$_c$) $\Leftrightarrow$ (d$_c$)". It follows from Lemma 3.2 (b) that an $\hat{h} > 0$ exists such that (a$_c$) $\Leftrightarrow$ (a$_\Delta$ holds for all $h \leq \hat{h}$). Applying Theorem 3.1 we get (a$_\Delta$) $\Leftrightarrow$ (d$_\Delta$) and finally, Lemma 3.1 yields (d$_\Delta$ holds for all $h \leq \hat{h}$) $\Leftrightarrow$ (d$_c$). □

Corollary 3.1 *Let* $\bar{x}_{\mathbb{Z}}$ *be a transversal homoclinic orbit of the map* $\varphi_n(\cdot, h)$. *Then* $\bar{x}_{\mathbb{Z}}$ *is a regular solution of the operator* Γ, *i.e.* $\Gamma(\bar{x}_{\mathbb{Z}}, h) = 0$ *and* $\Gamma_{x_{\mathbb{Z}}}(\bar{x}_{\mathbb{Z}}, h)$ *is a homeomorphism.*

4 Discretization by a one–step method

For a general one–step method, we prove a closeness result for approximate trajectories in our nonautonomous context. From this, we conclude our main theorem – the persistence of homoclinic orbits under one–step discretizations.

We consider a general one–step method

$$x_{n+1} = \psi_n(x_n, h), \quad x_n \in \mathbb{R}^k, \quad n \in \mathbb{Z} \tag{4.1}$$

with step size $h > 0$. The orbits of (4.1) are zeros of the operator

$$\tilde{\Gamma} : S_{\mathbb{Z}} \times \mathbb{R} \to S_{\mathbb{Z}}, \quad (x_{\mathbb{Z}}, h) \mapsto (x_{n+1} - \psi_n(x_n, h))_{n\in\mathbb{Z}}.$$

We assume consistency of order d as well as smoothness:

(A7) For any compact set $\mathcal{K} \subset \mathbb{R}^k$ there exist constants $C_2(\mathcal{K}), h_2(\mathcal{K}) > 0$ such that the consistency estimate of order $d \in \mathbb{N}$

$$\|\varphi_n(x, h) - \psi_n(x, h)\| \leq C_2(\mathcal{K})h^{d+1}$$

holds for all $n \in \mathbb{Z}$, $x \in \mathcal{K}$ and $0 < h \leq h_2(\mathcal{K})$.

(A8) Mixed derivatives of $\psi_n(x, h)$ up to order 3 exist. For any compact set $\mathcal{K} \subset \mathbb{R}^k$ the derivatives are continuous and uniformly bounded by some constant $\tilde{C}(\mathcal{K})$ in $\mathcal{K} \times (0, h_3(\mathcal{K})]$, with $0 < h_3(\mathcal{K})$ sufficiently small. Furthermore, $\psi_n(x, h)$ is $\mathcal{C}^d$ smooth in h and mixed derivatives $(\psi_n)^{(1,d)}_{x,h}(x, h)$ exist and satisfy the uniform Lipschitz estimate

$$\left\|(\psi_n)^{(1,d)}_{x,h}(x, \mu_1) - (\psi_n)^{(1,d)}_{x,h}(x, \mu_2)\right\| \leq C_3(\mathcal{K}) \|\mu_1 - \mu_2\|$$

for all $n \in \mathbb{Z}$, $x \in \mathcal{K}$ and $0 < \mu_{1,2} \leq h_3(\mathcal{K})$ with a constant $C_3(\mathcal{K}) > 0$.

The following Lemma summarizes closeness estimates between the h–flow and an h–step with (4.1). Garay proved in [9] closeness estimates for autonomous systems. With our uniformity Assumptions **(A7)** and **(A8)** Garay's approach immediately carries over to the nonautonomous case. For the readers convenience, we present a sketch of the proof.

Lemma 4.1 *Assume* **(A1)**, **(A7)** *and* **(A8)**. *Then for any compact set $\mathcal{K} \subset \mathbb{R}^k$ there exist constants $\tilde{C}(\mathcal{K}), C_4(\mathcal{K}), h_4(\mathcal{K}) > 0$ such that for all $x \in \mathcal{K}$ and $0 < h \leq h_4(\mathcal{K})$ with $h_4(\mathcal{K}) \leq h_{1,2,3}(\mathcal{K})$ the following statements hold true:*

(i) $\sup_{n\in\mathbb{Z}} \|(\varphi_n)_x(x, h) - (\psi_n)_x(x, h)\| \leq C_4(\mathcal{K})h^{d+1}$,

(ii) $\psi_n(x, h) = x + h\Delta_n(x, h)$ *where* $\Delta_n(x, h) := \int_0^1 (\psi_n)_h(x, sh)\mathrm{d}s$ *has the same smoothness properties as* ψ_n *except for losing one derivative with respect to* h. *Further, for* $r \in \{0, 1, 2\}$ *the following estimates are true:*

$$\sup_{n\in\mathbb{Z}} \|(\Delta_n)^{(r)}_x(x, h)\| \leq \tilde{C}(\mathcal{K}), \tag{4.2}$$

$$\sup_{n\in\mathbb{Z}} \|(\psi_n)_x(x, h)^{-1}\| \leq \frac{1}{1 - h\tilde{C}(\mathcal{K})}. \tag{4.3}$$

Proof With Taylor's formula at $h = 0$ and **(A8)** we get

$$\begin{aligned}&\varphi_n(x,h) - \psi_n(x,h)\\ &= \int_0^1 \left(\tfrac{(1-s)^{d-1}}{(d-1)!} (\varphi_n(x,sh) - \psi_n(x,sh))_h^{(d)} - (\varphi_n(x,0) - \psi_n(x,0))_h^{(d)} \right) \mathrm{d}s h^d\end{aligned}$$

for all $x \in \mathcal{K}$, $0 < h \le h_4(\mathcal{K})$. By differentiating this expression w.r.t. x and using **(A1)** and **(A7)** we get the estimate from (i). The second statement follows immediately from the mean value theorem. The estimate (4.2) is a direct consequence of **(A8)** and with the Banach–Lemma we obtain (4.3) for sufficiently small h. □

Now, we have all tools at hand to prove h^d–closeness between orbits of the continuous time system and orbits of the one–step discretization, see [30, Theorem 4.3] for a related result in autonomous systems.

Theorem 4.1 *Assume* **(A1)**, **(A6)**–**(A8)**. *Then there exist constants* $h_5, \delta > 0$ *such that for all* $0 < h \le h_5$ *the operator* $\tilde{\Gamma}(\cdot, h)$ *has a unique zero* $\tilde{y}_{\mathbb{Z}}(h)$ *in a* δ*–neighborhood of* $\bar{y}_{\mathbb{Z}}(h)$.
Furthermore, $\tilde{y}_{\mathbb{Z}}(h)$ *is a hyperbolic bounded trajectory of* (4.1) *that satisfies*

$$\sup_{n \in \mathbb{Z}} \|\tilde{y}_n(h) - \bar{y}_n(h)\| = \mathcal{O}(h^d). \tag{4.4}$$

Proof Let $\mathcal{K} \subset \mathbb{R}^k$ be compact and sufficiently large. We prove the statements from above by applying Lemma A.2 with the settings: $F = \tilde{\Gamma}$, $Y = S_{\mathbb{Z}}$, $\Lambda = \mathbb{R}^+$, $Z = S_{\mathbb{Z}}$ and $\bar{v}_0(h) = \bar{y}_{\mathbb{Z}}(h)$, $\delta_1 = \delta$ and $\delta_2 = h_5$.

We verify the assumptions of Lemma A.2 and first prove that $\tilde{\Gamma}(\cdot, h)$ for $0 < h \le h_5$ is invertible with uniformly bounded inverse.

From Lemma 4.1 we get the closeness estimate

$$\left\| \tilde{\Gamma}_{x_{\mathbb{Z}}}(x_{\mathbb{Z}}, h) - \Gamma_{x_{\mathbb{Z}}}(x_{\mathbb{Z}}, h) \right\| \le C_4(\mathcal{K}) h^{d+1} \tag{4.5}$$

for all $0 < h \le h_4(\mathcal{K})$ and $x_{\mathbb{Z}} \in \mathcal{K}^{\mathbb{Z}}$. Since $\Gamma_{x_{\mathbb{Z}}}(\bar{y}_{\mathbb{Z}}(h), h)$ is a homeomorphism for all $0 < h \le h_4(\mathcal{K})$, a possibly smaller bound $0 < h_5 \le h_4(\mathcal{K})$ exists such that $\tilde{\Gamma}_{x_{\mathbb{Z}}}(\bar{y}_{\mathbb{Z}}(h), h)$ is a homeomorphism for all $0 < h \le h_5$. Consequently, we obtain for any $\tilde{r}_{\mathbb{Z}}$, $r_{\mathbb{Z}} \in S_{\mathbb{Z}}$ unique solutions $\tilde{u}_{\mathbb{Z}}$, $u_{\mathbb{Z}} \in S_{\mathbb{Z}}$ of the inhomogeneous equations

$$\tilde{\Gamma}_{x_{\mathbb{Z}}}(\bar{y}_{\mathbb{Z}}(h), h)\tilde{u}_{\mathbb{Z}} = \tilde{r}_{\mathbb{Z}}, \quad \Gamma_{x_{\mathbb{Z}}}(\bar{y}_{\mathbb{Z}}(h), h) u_{\mathbb{Z}} = r_{\mathbb{Z}}.$$

From **(A6)** an exponential dichotomy of (3.3) with exponential rate $h\bar{\beta}$ and constant $\bar{K}$ follows. Applying Lemma A.1 together with an elementary estimate for the exponential, we obtain

$$\|u_{\mathbb{Z}}\| \le \bar{K} \frac{1 + e^{-h\bar{\beta}}}{1 - e^{-h\bar{\beta}}} \|r_{\mathbb{Z}}\| \le \frac{1}{\nu h} \|\Gamma_{x_{\mathbb{Z}}}(\bar{y}_{\mathbb{Z}}(h), h) u_{\mathbb{Z}}\| \tag{4.6}$$

with some constant $\nu > 0$ that does neither depend on h nor on $r_{\mathbb{Z}}$.

Combining (4.5) with (4.6) for $r_{\mathbb{Z}} := \Gamma_{x_{\mathbb{Z}}}(\bar{y}_{\mathbb{Z}}(h), h)\tilde{u}_{\mathbb{Z}}$, the estimate

$$\begin{aligned}
\|\tilde{r}_{\mathbb{Z}}\| &= \left\|\tilde{\Gamma}_{x_{\mathbb{Z}}}(\bar{y}_{\mathbb{Z}}(h), h)\tilde{u}_{\mathbb{Z}}\right\| \\
&\geq \|\Gamma_{x_{\mathbb{Z}}}(\bar{y}_{\mathbb{Z}}(h), h)\tilde{u}_{\mathbb{Z}}\| - \left\|(\Gamma_{x_{\mathbb{Z}}}(\bar{y}_{\mathbb{Z}}(h), h) - \tilde{\Gamma}_{x_{\mathbb{Z}}}(\bar{y}_{\mathbb{Z}}(h), h))\tilde{u}_{\mathbb{Z}}\right\| \\
&\geq \nu h \|\tilde{u}_{\mathbb{Z}}\| - C_4(\mathcal{K})h^{d+1}\|\tilde{u}_{\mathbb{Z}}\| \geq \frac{1}{2}\nu h \left\|\tilde{\Gamma}_{x_{\mathbb{Z}}}(\bar{y}_{\mathbb{Z}}(h), h)^{-1}\tilde{r}_{\mathbb{Z}}\right\| \qquad (4.7)
\end{aligned}$$

holds for all $0 < h \leq h_5$ with a possibly smaller h_5. Since (4.7) holds true for all $\tilde{r}_{\mathbb{Z}} \in S_{\mathbb{Z}}$ we conclude

$$\left\|\tilde{\Gamma}_{x_{\mathbb{Z}}}(\bar{y}_{\mathbb{Z}}(h), h)^{-1}\right\|^{-1} \geq \frac{\nu h}{2}. \qquad (4.8)$$

Next, we verify Assumption (A.3) of Lemma A.2 and define

$$\sigma(h) := \frac{\nu h}{2} \quad \text{and} \quad \kappa(h) := \frac{\sigma(h)}{2}. \qquad (4.9)$$

Lemma 4.1, **(A8)** and the mean value theorem yields

$$\begin{aligned}
&\left\|\tilde{\Gamma}_{x_{\mathbb{Z}}}(x_{\mathbb{Z}}, h) - \tilde{\Gamma}_{x_{\mathbb{Z}}}(\bar{y}_{\mathbb{Z}}(h), h)\right\| \leq h \left\|((\Delta_n)_x(\bar{y}_n(h), h) - (\Delta_n)_x(x_n, h))_{n\in\mathbb{Z}}\right\| \\
&\leq h \int_0^1 \left\|\Big((\Delta_n)_x^{(2)}(\bar{y}_n(h) + s(x_n - \bar{y}_n(h)), h)\Big)_{n\in\mathbb{Z}}\right\| \mathrm{d}s \, \|\bar{y}_{\mathbb{Z}}(h) - x_{\mathbb{Z}}\| \\
&\leq \tilde{C}(\mathcal{K})h \|\bar{y}_{\mathbb{Z}}(h) - x_{\mathbb{Z}}\| \qquad (4.10)
\end{aligned}$$

for all $x_{\mathbb{Z}} \in \mathcal{K}^{\mathbb{Z}}$ and $0 < h \leq h_4(\mathcal{K})$. Note that for sufficiently small δ the estimate $\tilde{C}(\mathcal{K})h\delta \leq \kappa(h)$ holds and using (4.8), Assumption (A.3) is confirmed for all $\|x_{\mathbb{Z}} - \bar{y}_{\mathbb{Z}}(h)\| \leq \delta$:

$$\begin{aligned}
\left\|\tilde{\Gamma}_{x_{\mathbb{Z}}}(x_{\mathbb{Z}}, h) - \tilde{\Gamma}_{x_{\mathbb{Z}}}(\bar{y}_{\mathbb{Z}}(h), h)\right\| &\leq \tilde{C}(\mathcal{K})h\delta \leq \kappa(h) < \sigma(h) = \frac{\nu h}{2} \\
&\leq \left\|\tilde{\Gamma}_{x_{\mathbb{Z}}}(\bar{y}_{\mathbb{Z}}(h), h)^{-1}\right\|^{-1}.
\end{aligned}$$

Assumption (A.4) of Lemma A.2 immediately follows from **(A7)** for sufficiently small h_5, $0 < h \leq h_5$:

$$\begin{aligned}
\left\|\tilde{\Gamma}(\bar{y}_{\mathbb{Z}}(h), h)\right\| &= \left\|\tilde{\Gamma}(\bar{y}_{\mathbb{Z}}(h), h) - \Gamma(\bar{y}_{\mathbb{Z}}(h), h)\right\| \\
&= \|(\varphi_n(\bar{y}_n(h), h) - \psi_n(\bar{y}_n(h), h))_{n\in\mathbb{Z}}\| \\
&\leq C_2(\mathcal{K})h^{d+1} \leq \frac{\nu h}{4}\delta \leq \frac{\sigma(h)}{2}\delta = (\sigma(h) - \kappa(h))\delta.
\end{aligned}$$

Thus, Lemma A.2 applies and guarantees the existence of a unique zero $\tilde{y}_{\mathbb{Z}}(h)$ of $\tilde{\Gamma}(\cdot, h)$ in a δ–neighborhood of $\bar{y}_{\mathbb{Z}}(h)$, satisfying the inequality (4.4)

$$\begin{aligned}
\|\tilde{y}_{\mathbb{Z}}(h) - \bar{y}_{\mathbb{Z}}(h)\| &\leq (\sigma(h) - \kappa(h))^{-1}\left\|\tilde{\Gamma}(\bar{y}_{\mathbb{Z}}(h), h)\right\| \\
&\leq \tfrac{4}{\nu h}C_2(\mathcal{K})h^{d+1} = \frac{4C_2(\mathcal{K})}{\nu}h^d \qquad (4.11)
\end{aligned}$$

for all $0 < h \leq h_5$.

Next, we prove hyperbolicity of this solution. In order to show that the variational equation, given in terms of the operator $\tilde{\Gamma}_{x_{\mathbb{Z}}}(\tilde{y}(h), h)$, has an exponential dichotomy on $\mathbb{Z}$, we apply the Roughness–Theorem A.1 with the settings: $A_n = (\varphi_n)_x(\bar{y}_n(h), h)$ and $E_n = (\psi_n)_x(\tilde{y}_n(h), h) - (\varphi_n)_x(\bar{y}_n(h), h)$.

With (4.10) and (4.11) it follows

$$\left\|\tilde{\Gamma}_{x_{\mathbb{Z}}}(\tilde{y}_{\mathbb{Z}}(h), h) - \tilde{\Gamma}_{x_{\mathbb{Z}}}(\bar{y}_{\mathbb{Z}}(h), h)\right\| \leq \tilde{C}(\mathcal{K}) h \frac{4C_3(\mathcal{K})}{\nu} h^d = \hat{C}(\mathcal{K}) h^{d+1}$$

and combining this result with (4.5) we obtain

$$\begin{aligned}
&\sup_{n\in\mathbb{Z}} \|(\psi_n)_x(\tilde{y}_n(h), h) - (\varphi_n)_x(\bar{y}_n(h), h)\| \\
&= \|\tilde{\Gamma}_{x_{\mathbb{Z}}}(\tilde{y}_{\mathbb{Z}}(h), h) - \Gamma_{x_{\mathbb{Z}}}(\bar{y}_{\mathbb{Z}}(h), h)\| \\
&\leq \|\tilde{\Gamma}_{x_{\mathbb{Z}}}(\tilde{y}_{\mathbb{Z}}(h), h) - \tilde{\Gamma}_{x_{\mathbb{Z}}}(\bar{y}_{\mathbb{Z}}(h), h)\| + \|\tilde{\Gamma}_{x_{\mathbb{Z}}}(\bar{y}_{\mathbb{Z}}(h), h) - \Gamma_{x_{\mathbb{Z}}}(\bar{y}_{\mathbb{Z}}(h), h)\| \\
&\leq (\hat{C}(\mathcal{K}) + C_4(\mathcal{K})) h^{d+1}. \qquad (4.12)
\end{aligned}$$

Following the proof of Lemma 4.1 (ii) we observe for h sufficiently small that

$$\sup_{n\in\mathbb{Z}} \|(\varphi_n)_x(\bar{y}_n(h), h)^{-1}\| \leq \frac{1}{1 - hC_1(\mathcal{K})}$$

and together with (4.12) this yields the estimate

$$\begin{aligned}
\frac{1}{2}\inf_{n\in\mathbb{Z}} \|(\varphi_n)_x(\bar{y}_n(h), h)^{-1}\|^{-1} &\geq \frac{1}{2}(1 - hC_1(\mathcal{K})) \geq (\hat{C}(\mathcal{K}) + C_4(\mathcal{K})) h^{d+1} \\
&\geq \sup_{n\in\mathbb{Z}} \|(\psi_n)_x(\tilde{y}_n(h), h) - (\varphi_n)_x(\bar{y}_n(h), h)\|
\end{aligned}$$

for h sufficiently small. This is the first Assumption (A.1) of the Roughness–Theorem A.1. For verifying the second Assumption (A.2), note that (3.3) has an exponential dichotomy on $\mathbb{Z}$ with data $(\bar{K}, h\bar{\beta}, Q_n^{s,u}(h))$ and observe

$$\left(\frac{1}{e^{\frac{h\bar{\beta}}{2}} - e^{-h\bar{\beta}}} + \frac{1}{e^{-\frac{h\bar{\beta}}{2}} - e^{-h\bar{\beta}}} + \frac{1}{e^{h\bar{\beta}} - e^{-\frac{h\bar{\beta}}{2}}}\right)^{-1} = \frac{3}{10}\bar{\beta} h + \mathcal{O}(h^2). \qquad (4.13)$$

As a consequence

$$\begin{aligned}
&\sup_{n\in\mathbb{Z}} \|(\psi_n)_x(\tilde{y}_n(h), h) - (\varphi_n)_x(\bar{y}_n(h), h)\| \leq (\hat{C}(\mathcal{K}) + C_4(\mathcal{K})) h^{d+1} \\
\leq &\frac{1}{2}\bar{K}^{-1}\left(\frac{1}{e^{\frac{h\bar{\beta}}{2}} - e^{-h\bar{\beta}}} + \frac{1}{e^{-\frac{h\bar{\beta}}{2}} - e^{-h\bar{\beta}}} + \frac{1}{e^{h\bar{\beta}} - e^{-\frac{h\bar{\beta}}{2}}}\right)^{-1}
\end{aligned}$$

holds true for h sufficiently small. Lemma A.1 applies and guarantees that the variational equation, given in terms of $\tilde{\Gamma}_{x_{\mathbb{Z}}}(\tilde{y}_{\mathbb{Z}}(h), h)$, has an exponential dichotomy on $\mathbb{Z}$ with constant $2\bar{K}+1$ and rate $\frac{h\bar{\beta}}{2}$. Thus, $\tilde{y}_{\mathbb{Z}}(h)$ is a hyperbolic bounded trajectory of the h–step method $\psi_{\mathbb{Z}}(\cdot, h)$ for all $0 < h \leq h_5$. $\square$

We exploit this result for analyzing discretized homoclinic orbits. Note that the application of a one–step method turns the equilibrium 0 into a bounded trajectory.

Corollary 4.1 *Assume* **(A1)**–**(A3)**, **(A7)** *and* **(A8)**. *Choose* h_2 *and* δ *as in Theorem 4.1. Then there exists a* $C > 0$, *such that for all* $0 < h \le h_5$ *a unique hyperbolic bounded trajectory* $\tilde{\xi}_{\mathbb{Z}}(h)$ *of* (4.1) *in a* δ*–neighborhood of the equilibrium* 0 *of* (2.1) *exists which satisfies*

$$\sup_{n\in\mathbb{Z}} \left\| \tilde{\xi}_n(h) - 0 \right\| \le Ch^d.$$

The variational equation, belonging to $\tilde{\Gamma}_{x_{\mathbb{Z}}}(\tilde{\xi}_{\mathbb{Z}}(h), h)$, *has an exponential dichotomy on* $\mathbb{Z}$ *with constant* $2K + 1$ *and rate* $\frac{h\beta}{2}$.

Further assume **(A4)** *and* **(A5)**. *Then there exists a unique hyperbolic bounded trajectory* $\tilde{x}_{\mathbb{Z}}(h)$ *of* (4.1) *in a* δ*–neighborhood of the transversal homoclinic orbit* $\bar{x}_{\mathbb{Z}}(h)$ *of the* h*–flow, which satisfies*

$$\sup_{n\in\mathbb{Z}} \|\tilde{x}_n(h) - \bar{x}_n(h)\| \le Ch^d.$$

Furthermore, there exists an $N \in \mathbb{Z}^+$, *such that*

$$\sup_{n\in J^\pm} \|\tilde{x}_n(h) - \tilde{\xi}_n(h)\| \le 3Ch^d \tag{4.14}$$

holds with $J^+ := [N, \infty) \cap \mathbb{Z}$, $J^- := (-\infty, -N] \cap \mathbb{Z}$.

Proof It remains to prove the estimate (4.14) for sufficiently large $|n|$, $n \in \mathbb{Z}$:

$$\begin{aligned} &\sup_{n\in J^\pm} \|\tilde{x}_n(h) - \tilde{\xi}_n(h)\| \\ &\le \sup_{n\in\mathbb{Z}} \|\tilde{x}_n(h) - \bar{x}_n(h)\| + \sup_{n\in J^\pm} \|\bar{x}_n(h) - 0\| + \sup_{n\in\mathbb{Z}} \|0 - \tilde{\xi}_n(h)\| \le 3Ch^d. \end{aligned}$$

□

From the previous results, we already know that the tails of the discretized hyperbolic bounded trajectories $\tilde{x}_{\mathbb{Z}}(h)$ and $\tilde{\xi}_{\mathbb{Z}}(h)$ of (4.1) stay in a common small neighborhood. In the following we show that these trajectories are indeed homoclinic toward each other for all $0 < h \le h_5$. This can be achieved by establishing the identity

$$\lim_{n\to\pm\infty} \left\| \tilde{x}_n(h) - \tilde{\xi}_n(h) \right\| = 0.$$

The next lemma states that if two hyperbolic bounded trajectories stay in a sufficiently small common neighborhood, then they converge towards each other. Note that a related result for the autonomous case can be found in [24, Lemma 5.3].

Lemma 4.2 *Assume that $f_n \in \mathcal{C}^1(\mathbb{R}^k, \mathbb{R}^k)$ for $n \in \mathbb{Z}$ and let $\xi_{\mathbb{Z}}$ be a bounded trajectory of the difference equation*

$$x_{n+1} = f_n(x_n), \quad n \in \mathbb{Z}. \tag{4.15}$$

Further assume that $(f_n)_x$ is uniformly Lipschitz with constant L in a neighborhood of $\xi_{\mathbb{Z}}$ for all $n \in \mathbb{Z}$ and that the variational equation

$$u_{n+1} = (f_n)_x(\xi_n)u_n, \quad n \in \mathbb{Z} \tag{4.16}$$

has an exponential dichotomy on $\mathbb{Z}$ with data $(K, \alpha, P_n^{s,u})$. Fix $n_1 \in \mathbb{N}$ and let $x_{\mathbb{Z}}$ be a second bounded trajectory of (4.15), satisfying the following estimates with some constant $0 < \beta < \alpha$:

$$\|(x_n - \xi_n)_{n\in\mathbb{T}}\| \le L^{-1} \inf_{n\in\mathbb{T}} \|(f_n)_x(\xi_n)^{-1}\|^{-1}, \tag{4.17}$$

$$\|(x_n - \xi_n)_{n\in\mathbb{T}}\| \le L^{-1}K^{-1}\left(\frac{1}{e^{\beta} - e^{-\alpha}} + \frac{1}{e^{-\beta} - e^{-\alpha}} + \frac{1}{e^{\alpha} - e^{-\beta}}\right)^{-1}, \tag{4.18}$$

for $\mathbb{T} \in \{(-\infty, n_1] \cap \mathbb{Z}, [n_1, \infty) \cap \mathbb{Z}\}$.

Then there exists a constant $\tilde{C} > 0$ such that the exponential estimate

$$\|x_n - \xi_n\| \le \tilde{C}e^{-\beta|n-n_1|} \tag{4.19}$$

holds for all $n \in \mathbb{T}$.

Proof First we define $z_n := x_n - \xi_n$ for $n \in \mathbb{T}$ and get with the mean value theorem

$$\begin{aligned} z_{n+1} = x_{n+1} - \xi_{n+1} &= f_n(x_n) - f_n(\xi_n) \\ &= f_n(z_n + \xi_n) - f_n(\xi_n) = \int_0^1 (f_n)_x(\xi_n + sz_n)\mathrm{d}s z_n. \end{aligned}$$

By defining $B_n = \int_0^1 (f_n)_x(\xi_n + sz_n)\mathrm{d}s$ we see that $z_{\mathbb{T}}$ is a bounded solution of

$$u_{n+1} = B_n u_n, \quad n \in \mathbb{T}. \tag{4.20}$$

To finish the proof, we show that (4.20) has an exponential dichotomy on $\mathbb{T}$ with data $(2K + 1, \beta, Q_n^{s,u})$.

Assume this dichotomy is already known. Then we get $z_n = Q_n^u z_n$ for $n \in \mathbb{T}_1 = (-\infty, n_1] \cap \mathbb{Z}$ and $z_n = Q_n^s z_n$ for $n \in \mathbb{T}_2 = [n_1, \infty) \cap \mathbb{Z}$ since $z_{\mathbb{T}}$ is a bounded solution of (4.20). Denote by $\Phi(\cdot, \cdot)$ the corresponding solution operator, then

$$\|z_n\| = \|\Phi(n, n_1)Q_{n_1}^{s,u} z_{n_1}\| \le (2K + 1)e^{-\beta|n-n_1|}\|z_{n_1}\|$$

for $n \in \mathbb{T}_{2,1}$ which completes the proof of (4.19).

For proving an exponential dichotomy of (4.20), we start with (4.16) that already has an exponential dichotomy and apply the Roughness–Theorem A.1. To verify its assumptions, we use the estimate

$$\begin{aligned}\|B_n - (f_n)_x(\xi_n)\| &\le \int_0^1 \|(f_n)_x(\xi_n + s z_n) - (f_n)_x(\xi_n)\| \,\mathrm{d}s \\ &\le L \int_0^1 \|s z_n\| \mathrm{d}s \le \frac{1}{2} L \|z_n\| \text{ for all } n \in \mathbb{T}.\end{aligned}$$

Then Assumption (A.1) of the Roughness–Theorem A.1 directly follows from (4.17) and (A.2) from (4.18). □

Our next step is to show that discretized homoclinic trajectories converge towards each other. For this task, Lemma 4.2 is applied to the one–step method $\psi_{\mathbb{Z}}(\cdot, h)$ and the hyperbolic bounded trajectories $\tilde{\xi}_{\mathbb{Z}}(h)$ and $\tilde{x}_{\mathbb{Z}}(h)$.

From Corollary 4.1 we know that the variational equation, belonging to $\tilde{\Gamma}_{x\mathbb{Z}}(\tilde{\xi}_{\mathbb{Z}}(h), h)$, has an exponential dichotomy on $\mathbb{Z}$ with constant $2K+1$ and dichotomy rate $\frac{h\beta}{2}$. Let $\mathcal{K} \subset \mathbb{R}^k$ be compact and sufficiently large such that $\tilde{\xi}_{\mathbb{Z}}(h), \tilde{x}_{\mathbb{Z}}(h) \in \mathcal{K}^{\mathbb{Z}}$. Then the Lipschitz constant of $(\psi_n)_x$ is $L := h\tilde{C}(\mathcal{K})$, see equation (4.10). The first Assumption (4.17) of Lemma 4.2 for $\mathbb{T}_{1,2} := J^{\pm}$ follows with (4.3) and (4.14) for h sufficiently small:

$$\begin{aligned}\sup_{n \in J^{\pm}} \|\tilde{x}_n(h) - \tilde{\xi}_n(h)\| &\le 3Ch^d \le h^{-1}\tilde{C}(\mathcal{K})^{-1}(1 - h\tilde{C}(\mathcal{K})) \\ &\le L^{-1} \inf_{n \in \mathbb{Z}} \|(\psi_n)_x(\tilde{\xi}_n(h), h)^{-1}\|^{-1}.\end{aligned}$$

The second one (4.18) is fulfilled with $\bar{\beta} := \frac{\beta}{2}$ since

$$\begin{aligned}&\sup_{n \in J^{\pm}} \|\tilde{x}_n(h) - \tilde{\xi}_n(h)\| \le 3Ch^d \le \frac{h^{-1}\tilde{C}(\mathcal{K})^{-1}}{2K+1} 3C(2K+1)\tilde{C}(\mathcal{K})h^2 \\ &\le \frac{L^{-1}}{2K+1} \left(\frac{1}{e^{\frac{h\bar{\beta}}{2}} - e^{-h\bar{\beta}}} + \frac{1}{e^{-\frac{h\bar{\beta}}{2}} - e^{-h\bar{\beta}}} + \frac{1}{e^{h\bar{\beta}} - e^{-\frac{h\bar{\beta}}{2}}} \right)^{-1}\end{aligned}$$

follows from (4.14) and (4.13) for h sufficiently small. Now we apply Lemma 4.2 and get a constant $C_5 > 0$ such that

$$\|\tilde{x}_n(h) - \tilde{\xi}_n(h)\| \le C_5 e^{-\frac{h\beta}{4}|n-N|} \tag{4.21}$$

for all $n \in J^{\pm}$.

Summarizing these results we have seen that bounded trajectories in continuous time lead to bounded trajectories in discrete time, staying close to each other. Furthermore, if the tails of two trajectories of a nonautonomous system lie for all future (backward) times in a sufficiently small neighborhood, then they converge exponentially fast towards each other in forward (backward) time. As a consequence, homoclinic orbits stay homoclinic under discretization by a one–step method. This is the message of our main result:

Theorem 4.2 *Let $\bar{x}(\cdot)$ be a homoclinic orbit of the continuous time system* (2.1) *w.r.t. the fixed point* 0 *and assume that our Assumptions* **(A1)–(A5)**, **(A7)** *and* **(A8)** *are satisfied. Then we find constants $\bar{h}, C > 0$, such that two hyperbolic bounded trajectories $\tilde{\xi}_{\mathbb{Z}}(h)$ and $\tilde{x}_{\mathbb{Z}}(h)$ of the one–step approximation* (4.1) *exist which satisfy*

$$\sup_{n\in\mathbb{Z}} \|\tilde{\xi}_n(h) - 0\| \le Ch^d, \quad \sup_{n\in\mathbb{Z}} \|\tilde{x}_n(h) - \bar{x}_n(h)\| \le Ch^d,$$
$$\lim_{n\to\pm\infty} \left\|\tilde{x}_n(h) - \tilde{\xi}_n(h)\right\| = 0 \quad \text{for all } 0 < h < \bar{h}.$$

5 Applications

In this section we construct a two–dimensional example with an explicitly known homoclinic orbit. We compare orbits of a one–step method with the exact ones and numerically verify our error estimates for various step sizes.

For illustrating transversality of the computed orbits we look at the corresponding stable and unstable fiber bundles of the one–step discretization. We propose an algorithm for the approximation of one–dimensional stable fibers in a two–dimensional system that does not need the inverse map (which does not exist in general). The presented approach is a nonautonomous generalization from techniques that are introduced in [6].

Periodic forcing of an autonomous ODE leads to a special class of nonautonomous systems. We construct a model of this type and discuss the underlying autonomous dynamics and their influence on invariant fiber bundles along a homoclinic orbit.

Finally, a two–dimensional continuous time model from mathematical biology is introduced that is nonautonomous due to time variant environmental influences. For its time discretization we compute a homoclinic orbit as well as invariant fiber bundles.

5.1 An artificial example with explicitly known homoclinic orbits

We start with the Hamiltonian system

$$\dot{x} = f(x) = \begin{pmatrix} x_2 \\ x_1^2 - 4 \end{pmatrix},$$

which has the homoclinic orbit

$$\hat{x}(t) = 2(1 - 3\text{sech}^2(t), 6\text{sech}^2(t)\tanh(t))$$

with respect to the fixed point $(2, 0)$, see [3, Section 11.2.2], [10, Section 7.3].

To construct a nonautonomous example, we first shift the fixed point to $(0, 0)$. This leads us to the new system

$$\dot{x} = f(x) = \begin{pmatrix} x_2 \\ x_1^2 + 4x_1 \end{pmatrix} \tag{5.1}$$

with corresponding homoclinic orbit

$$\bar{x}(t) = 6(-\mathrm{sech}^2(t), 2\mathrm{sech}^2(t)\tanh(t)). \tag{5.2}$$

Next we add a nonautonomous term as follows

$$\begin{aligned} \dot{x} = g(x,t) &:= f(x) + \begin{pmatrix} x_1(x_1 - \bar{x}_1(t)) \\ x_2(x_2 - \bar{x}_2(t)) \end{pmatrix} \\ &= \begin{pmatrix} x_2 + x_1^2 + 6\mathrm{sech}^2(t)x_1 \\ x_1^2 + 4x_1 + x_2^2 - 12\mathrm{sech}^2(t)\tanh(t)x_2 \end{pmatrix}. \end{aligned} \tag{5.3}$$

Obviously, $(0,0)$ is for all $t \in \mathbb{R}$ a fixed point; furthermore, (5.2) is still a homoclinic orbit w.r.t. $(0,0)$ of this new system.

For a one–step discretization, we choose Heun's method with step size h which has order $d = 2$ and obtain the discrete time system

$$x_{n+1} = F_n(x_n) := x_n + \frac{h}{2}\left(g(x_n,t_n) + g(x_n + hg(x_n,t_n), t_{n+1})\right), \quad n \in \mathbb{Z}. \tag{5.4}$$

Tools for the numerical approximation of homoclinic orbits in nonautonomous systems have been proposed in [13, 16]. The key idea lies in introducing boundary value problems to obtain error controlled orbit segments on a finite time interval. More precisely, we compute an orbit segment $(\tilde{x}_{n_-}, \ldots, \tilde{x}_{n_+})$ by solving the periodic boundary value problem

$$\begin{pmatrix} x_{n_-+1} - F_{n_-}(x_{n_-}) \\ \vdots \\ x_{n_+} - F_{n_+-1}(x_{n_+-1}) \\ x_{n_-} - x_{n_+} \end{pmatrix} = \begin{pmatrix} 0 \\ \vdots \\ \vdots \\ 0 \end{pmatrix}, \tag{5.5}$$

using Newton's method with an appropriate initial guess. For the model (5.4), we start with the exact orbit (5.2). Note that the sparse structure of the derivative allows efficient computations. We solve (5.5) on the time–interval $[-30, 30]$ with the step size $h = 0.03$, i.e. $n_\pm = \pm 1000$. Figure 5.1 shows the orbit with time dependence (right) and without it (left).

Theorem 4.2 states that the maximal error $e_{\mathbb{Z}}(h) := \max_{n\in\mathbb{Z}} \|\tilde{x}_n - \bar{x}(hn)\|$ that occurs by approximating the original orbit using an h–step method of order d is less than Ch^d, with some constant $C > 0$. Furthermore, the computation of finite orbit segments by solving (5.5) introduces a second error. A precise analysis of this second error, cf. [16, Theorem 5], reveals that its maxima occur at the end points of the finite interval whereas this error decreases exponentially fast towards the midpoint. Thus, we avoid secondary errors by computing a solution of (5.5) on the time–interval $[-30, 30]$ and determine the maximal error $e(h) := \max_{n\in[-\frac{5}{h},\frac{5}{h}]\cap\mathbb{Z}} \|\tilde{x}_n - \bar{x}(hn)\|$ only on the center $[-5, 5]$. Figure 5.2 illustrates the numerical output of this procedure for various step sizes from 0.00005 up to 0.04 in a double logarithmic scale. The slope of the graph represents the exponent d. In Figure 5.2 it is 1.9930 in accordance with Theorem 4.2.

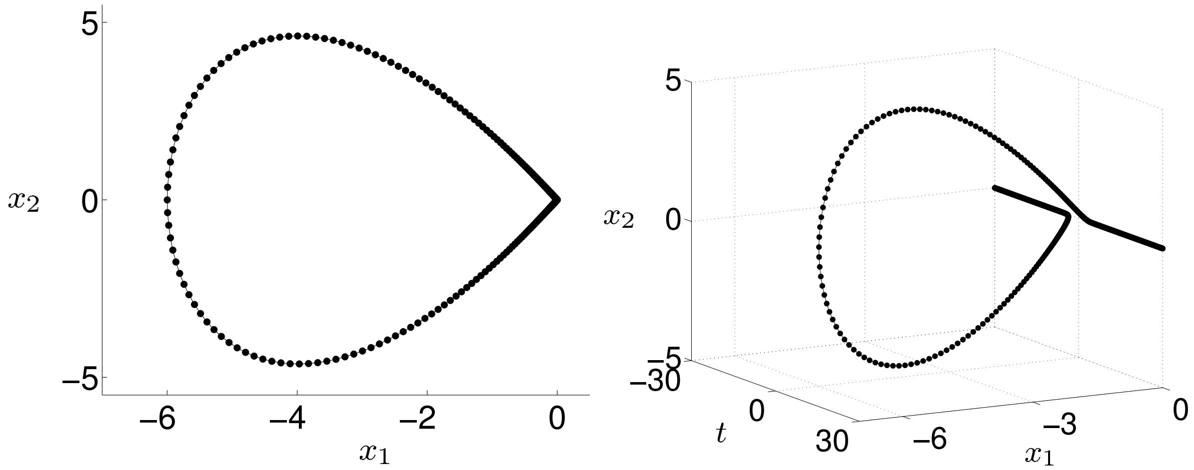

Fig. 5.1 Projection onto the x_1–x_2–plane (left), orbit with time dependence (right).

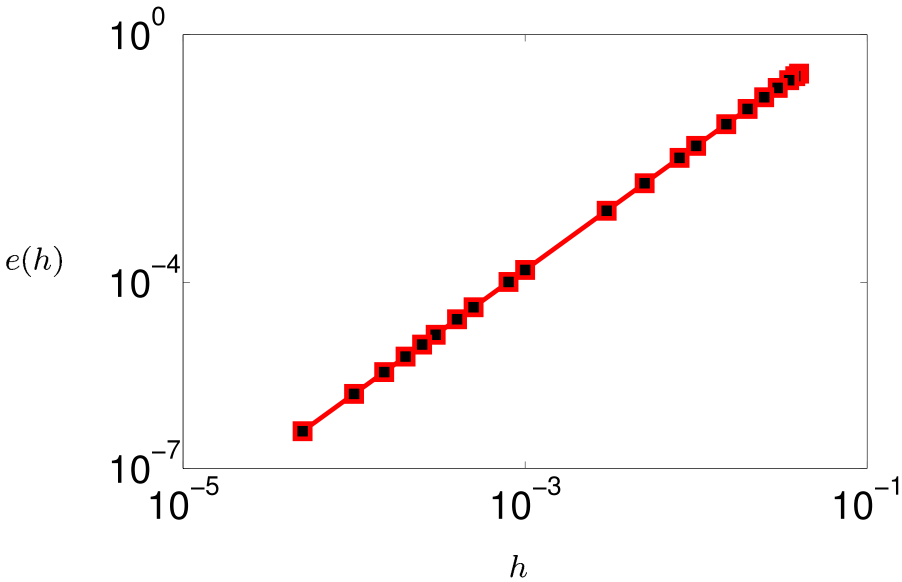

Fig. 5.2 Maximal error between exact and numerically approximated orbits.

5.2 An algorithm for computing stable fiber bundles

In autonomous systems, stable and unstable manifolds of a hyperbolic fixed point are important sources for understanding underlying dynamics. Numerical tools for their computation are often based on continuation techniques, see for example [20]. If the system is noninvertible, stable sets cannot be computed via backward iteration. To avoid this problem, the authors of [6] proposed a refined approach – the so called search circle algorithm – for computing stable sets without applying the inverse mapping.

The method that we introduce here generalizes these ideas to the nonautonomous case

$$x_{n+1} = f_n(x_n), \quad f_n(0) = 0 \text{ for all } n \in \mathbb{Z}, \tag{5.6}$$

where 0 is a hyperbolic fixed point.

The algorithm chooses the first point on a linear approximation of the stable fiber, i.e. its tangent space. This subspace can formally be expressed as the stable subspace of an exponential dichotomy, which the variational equation

$$u_{n+1} = Df_n(0)u_n, \quad n \in \mathbb{Z}$$

possesses due to our hyperbolicity assumption, cf. [13, Theorem 3.5]. Indeed, these subspaces are numerically accessible, using tools that have been developed in [14, 15].

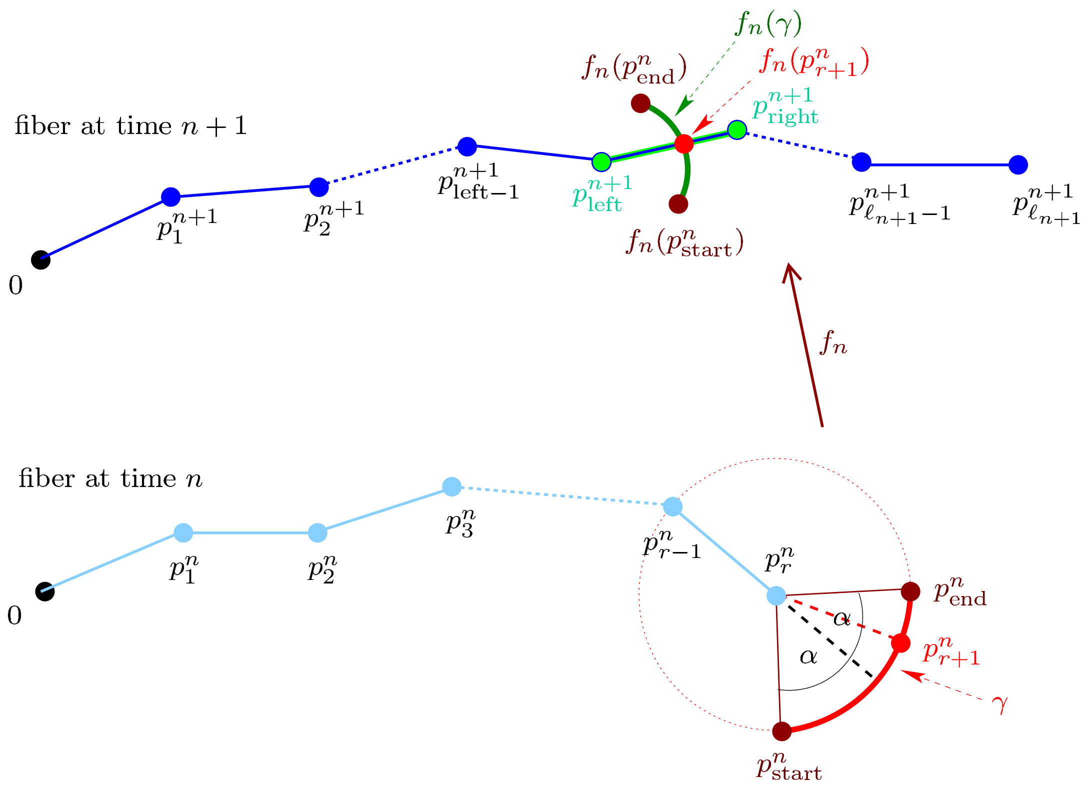

Fig. 5.3 Approximation of stable fiber bundles.

One step of the algorithm works as follows. Assume we already have an approximation of the $(n+1)$–th fiber, given by the set of points $M^{n+1} := \{p_1^{n+1}, \dots, p_{\ell_{n+1}}^{n+1}\}$ that are marked in blue in Figure 5.3. Further assume that the points $p_1^n, \dots, p_r^n$ on the n–th fiber have also been computed (light blue data in Figure 5.3). We search for the next point p_{r+1}^n (red) on a circular segment γ, marked in red in Figure 5.3. Then, its boundary points p_{end}^n and p_{start}^n are mapped by f_n (dark red data). If the angle α of the circular segment is chosen appropriately, $f_n(p_{\mathrm{start}}^n)$ and $f_n(p_{\mathrm{end}}^n)$ lie on different sides of the $(n+1)$–th fiber and thus, $f_n(\gamma)$ has a common intersection with this fiber. For its approximation, we first detect the neighboring points p_{left}^{n+1}, $p_{\mathrm{right}}^{n+1} \in M^{n+1}$ (green in Figure 5.3) and then calculate the point of intersection between the line segment $\overline{p_{\mathrm{left}}^{n+1} p_{\mathrm{right}}^{n+1}}$ and $f_n(\gamma)$ using bisection. Its pre–image under f_n is the next point p_{r+1}^n on the n–th fiber.

In case $f_n(\gamma)$ lies beyond the $(n+1)$–th fiber, the continuation of the n–th fiber stops and we proceed with the $(n-1)$–th fiber. Note that the first fibers that we compute in this way are rather short, but expanding dynamics on the stable fibers – in backward time – lead to an increase of length if n decreases. Figure 5.4 illustrates this increase of length for our artificial example from Section 5.1. In the left diagram the stable fibers are extremely close to each other. To reveal the differences we rotate the highlighted area of the left picture and show its zoom in the right part of Figure 5.4. The bottom stable fiber (darkest shade of green) in Figure 5.4 is the first computed one and belongs to time $70h$; the last computed one is the 65-th fiber at the top (lightest shade of green). Particularly, the shades of green from dark to light show the order, in which stable fibers are calculated by our algorithm.

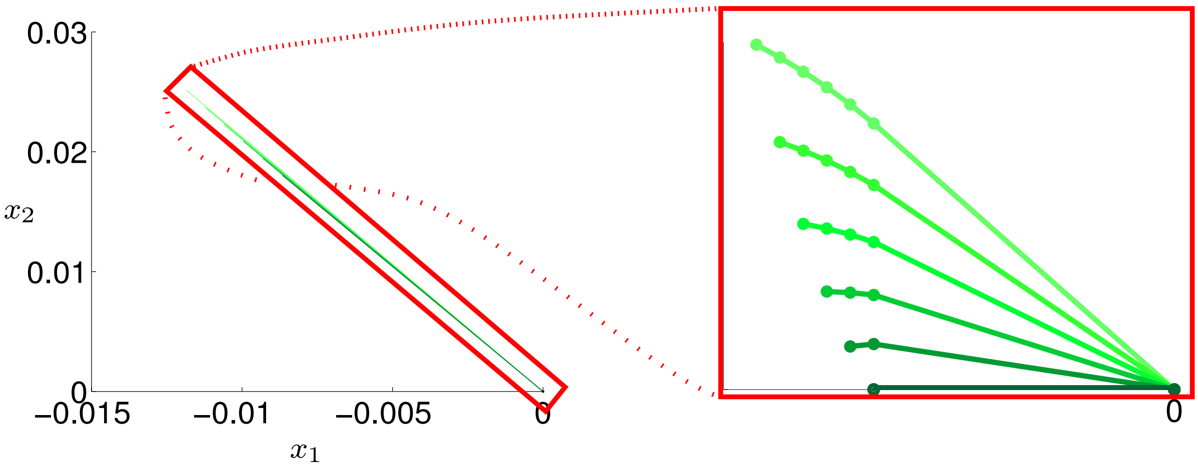

Fig. 5.4 Computation of stable fibers for (5.3), (5.4) with $h = 0.04$.

We finally note that details on the choice of the search angle α and on techniques for step size control have a similar implementation in autonomous systems and can be found in [6].

The computation of unstable fiber bundles is not so involved. One can choose points on the tangent space and iterate them in forward time, jumping in this way from fiber to fiber (neglecting small approximation errors).

The upper diagrams in Figure 5.5 show for the model from Section 5.1 a homoclinic orbit together with transversally intersecting fibers. The left panel illustrates them at time $20h$ and the right panel pictures them at the next time instance $21h$. The stable fibers (green) are computed with the algorithm from above while the unstable fibers (red) are approximated by forward iteration. The lower diagram visualizes transversally intersecting fiber bundles on the time interval $[-30h, 30h]$.

This orbit is truly nonautonomous, since two fibers at different times do not coincide.

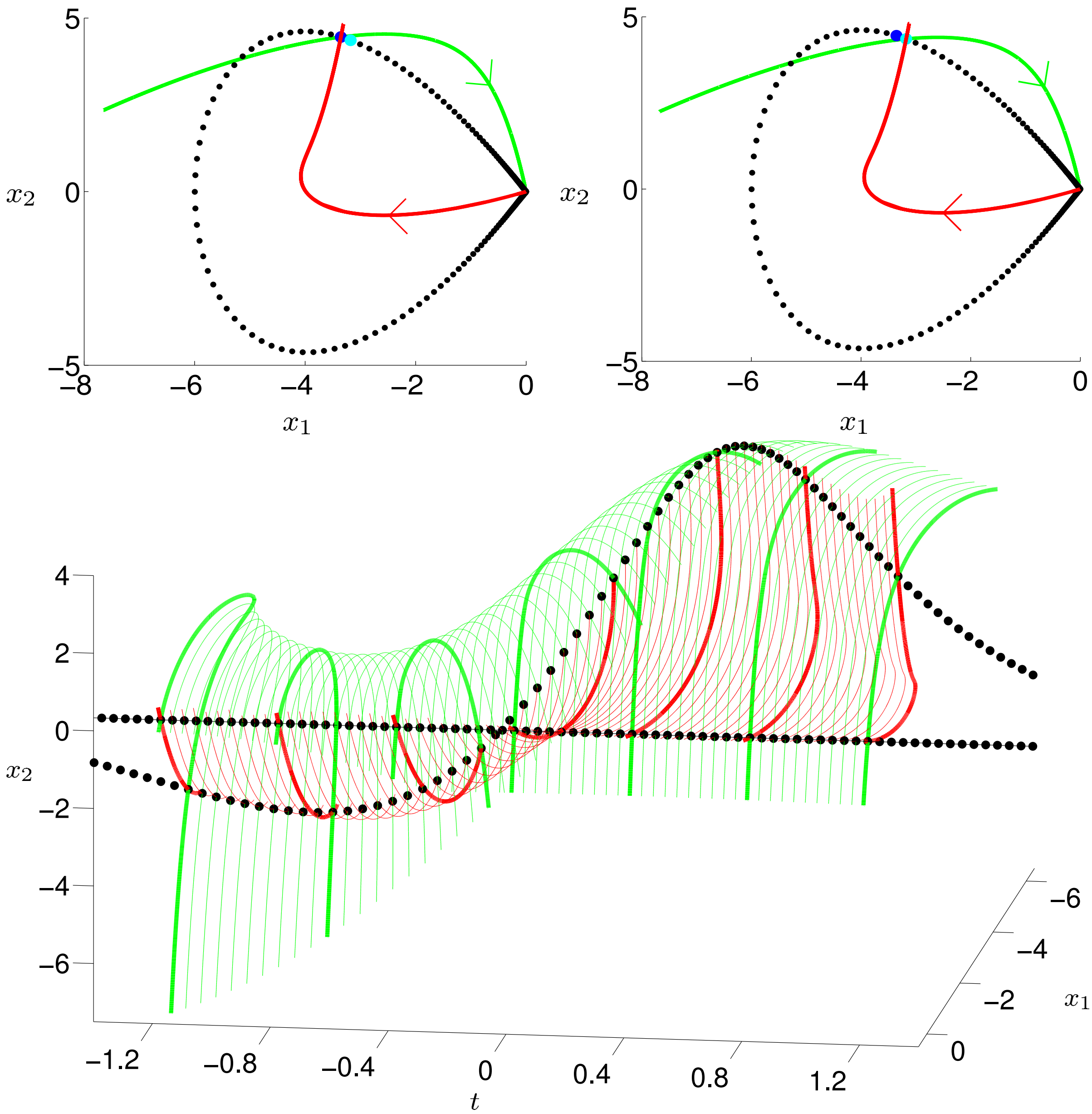

Fig. 5.5 Homoclinic orbit and transversally intersecting fiber bundles of (5.3), (5.4) with $h = 0.04$.

5.3 A periodic nonautonomous ODE

In τ–periodic ODEs, stable (and unstable) fibers of a fixed point at times t and $t+\tau$, $t \in \mathbb{R}$ coincide. For an illustration we modify (5.1) to the $\tau = \pi$–periodic model

$$\dot{x} = f(x,t) = \begin{pmatrix} -(1+0.3\sin(2t))x_2 \\ x_1^2 + x_1 \end{pmatrix}. \tag{5.7}$$

Discretizing this system with Heun's method and step size $h = \frac{\pi}{30}$ leads to a 30–periodic difference equation of the form

$$x_{n+1} = g_n(x_n), \quad g_n = g_{n+30}, \quad n \in \mathbb{Z}. \tag{5.8}$$

This discrete time system exhibits a homoclinic orbit w.r.t. the fixed point $(-1,0)$, see Figure 5.6 for an illustration. We further observe that stable and unstable fibers intersect transversally at every 30th point along the orbit. Stable and unstable fibers at time $20h$ are depicted in Figure 5.6. For their computation, we apply the algorithm from Section 5.2.

Note that alternatively, autonomous tool for computing homoclinic orbits from [4] as well as the search circle algorithm, introduced in [6], are directly applicable to $G_n := g_{n+29} \circ \cdots \circ g_n$, $n \in \mathbb{Z}$ fixed. We do not follow this route, since this problem typically has a worse condition number than the nonautonomous equation (5.8).

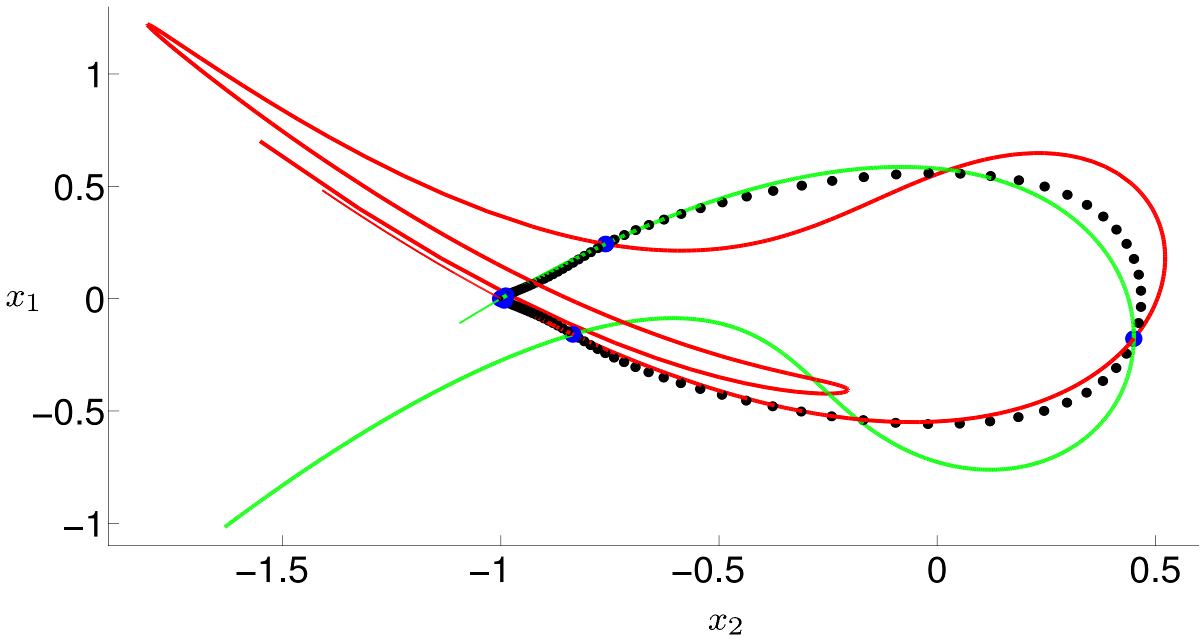

Fig. 5.6 Homoclinic orbit segment on the time interval $[-200h, 200h] \cap h\mathbb{Z}$ of (5.7) and the fibers at time $(20 + 30n)h$, $n \in [-7, 6] \cap \mathbb{Z}$.

5.4 An example from mathematical biology

Let us apply our techniques to a more realistic model from mathematical biology. The dynamics of the growth of algea and zooplankton, typically Daphnia, is presented in [26] with the help of a periodically forced predator–prey system. The authors introduce a 2–dimensional ODE

$$\begin{aligned} \tfrac{\mathrm{d}A}{\mathrm{d}t} &= 0.5A\left(1 - \tfrac{A}{10}\right) - 0.4Z\left(\tfrac{A}{A+0.6}\right) + 0.01(10 - A), \\ \tfrac{\mathrm{d}Z}{\mathrm{d}t} &= 0.24Z\tfrac{A}{A+0.6} - 0.15Z - E\tfrac{Z^2}{Z^2+0.5^2}, \end{aligned} \tag{5.9}$$

where (A) describes the amount of edible algea and (Z) the amount of large herbivorous zooplankton. The growth of zooplankton is influenced by the fish population and some other environmental terms (E). Our first step is to search for homoclinic structures in the autonomous system (5.9), see [26, Figure 6b], which can be found for

$$E := 0.0784372294995495865\ldots$$

Next we add a time–dependent perturbation to E reflecting time dependent environmental influences. Choosing

$$E(t) := 0.0784372294995495865 + \exp(-0.2t^2)$$

(5.9) is a continuous time nonautonomous 2–dimensional ODE of the form $\dot{x} = g(x,t)$ with $x := \begin{pmatrix} A & Z \end{pmatrix}^T$. We start with an analysis of the underlying dynamics by searching for homoclinic structures. To study this we are looking at the discretized system. For the one–step discretization $x_{n+1} = F_n(x_n)$ of the system we take Heun's method (5.4). First we compute a bounded trajectory $\hat{x}_{[n_-,n_+]}$ of (5.4) replacing the fixed point from the autonomous case. For this task, we solve, as in Section 5.1, the periodic boundary value problem (5.5) on the time–interval $[-1750, 1750]$ with step size $h = 0.5$, i.e. $n_\pm = \pm 3500$. Using this bounded solution $\hat{x}_{[n_-,n_+]}$ the transformed system

$$y_{n+1} = G_n(y_n),\ G_n(y_n) := F_n(y_n + \hat{x}_n) - \hat{x}_{n+1},\ n \in [n_-, n_+ - 1] \tag{5.10}$$

has $(0,0)$ as an n independent fixed point.

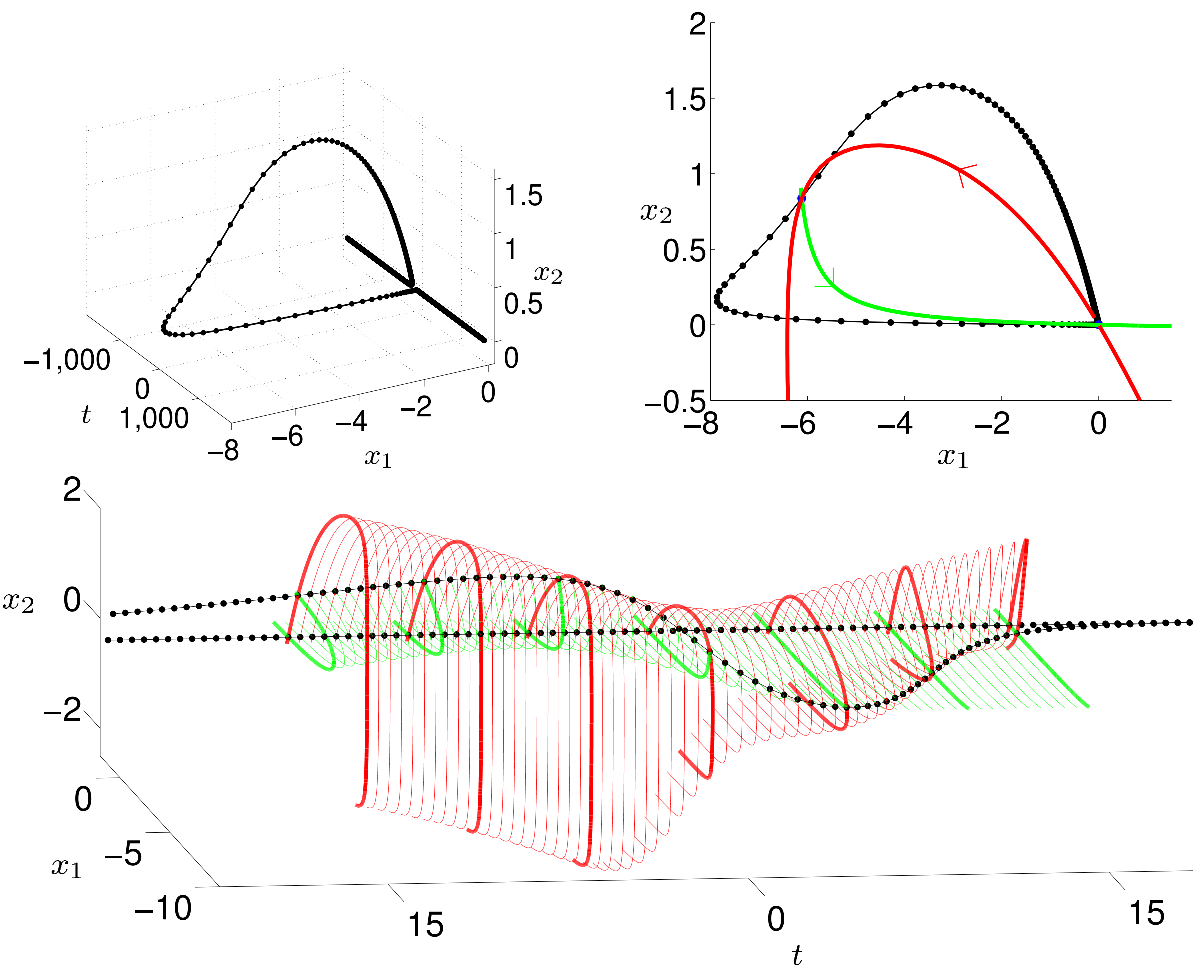

Fig. 5.7 Homolinic orbit of (5.10) with $h = 0.5$ (top left) and transversally intersecting fiber bundles (right and bottom).

To obtain a homoclinic orbit w.r.t. the fixed point $(0,0)$, see Figure 5.7 (left), we solve the periodic boundary value problem (5.5) with $G_n(\cdot)$ instead of $F_n(\cdot)$ and initial value

$$(0,\dots,0,x_n,G_n(x_n),G_{n+1}G_n(x_n),\dots,G_{n+249}G_{n+248}\cdots G_n(x_n),0,\dots,0),$$
$$n=-125,\ x_{-125}=\begin{pmatrix}-0.081\\ 0.096\end{pmatrix}.$$

In the top right diagram of Figurer 5.7 the stable (green) and unstable (red) fibers at time 0 are plotted. The stable fiber is approximated with the algorithm introduced in Section 5.2. The fibers intersect each other transversally in a single point. This is also the case for fibers in the time interval $[-30h,30h]$, see the lower diagram in Figure 5.7. For the original continuous time system, this is a strong evidence for transversal homoclinic trajectories, satisfying **(A5)**.

6 Conclusion

We studied transversal homoclinic orbits in nonautonomous ODEs. Transversality can be characterized by an exponential dichotomy of the corresponding variational equation. An equivalent, but more geometric interpretation is given in terms of transversally intersecting fiber bundles along the homoclinic orbit. These properties carry over to the h-flow and are used for proving existence of homoclinic orbits of one–step discretizations. Furthermore, closeness estimates have been established.

It is important to keep in mind that in nonautonomous ODEs, stable and unstable fibers of a fixed point typically intersect each other transversally at any fixed time. If the system is τ-periodic, then one observes an infinite number of isolated points of intersection along a homoclinic orbit and the τ-flow defines an autonomous system. On the other hand, intersecting stable and unstable manifolds in autonomous systems have a whole orbit in common.

For autonomous ODEs, the existence of nondegenerate homoclinic orbits is of codimension 1, see [3, Section 6]. Contrary to this result, the existence of transversal homoclinic orbits in nonautonomous ODEs is of codimension 0. Thus, these objects can be found for a wide range of parameters in various models.

For an illustration of stable and unstable fiber bundles, we restrict ourselves in this paper to the two–dimensional plane and propose adequate numerical tools. Note that an alternative algorithm for computing stable fibers has been introduced in [17]. This algorithm is based on computing zero contours of a particular operator and it applies to two and three–dimensional nonautonomous, noninvertible maps.

Finally, we point out that all theorems presented in this article as well as the boundary value approach (5.5) for computing homoclinic orbit segments are formulated in arbitrary space dimensions.

A Appendix

A.1 Exponential dichotomy

Consider a nonautonomous linear ODE or difference equation, for which the solution operator $S(\cdot,\cdot)$ is well defined on $J \times J$, where J is an interval of $\mathbb{R}$ or $\mathbb{Z}$, respectively.

Definition A.1 The equation has an **exponential dichotomy** on J if there exist constants $K, \alpha > 0$ and families of projectors $P_n^{s,u}$, $n \in J$ with $I = P_n^s + P_n^u$ for all $n \in J$ such that the invariance condition

$$P_n^{s,u} S(n,m) = S(n,m) P_m^{s,u} \text{ for all } n, m \in J$$

holds true as well as the following estimates for $n \geq m$, $n, m \in J$:

$$\|S(n,m)P_m^s\| \leq K e^{-\alpha(n-m)}, \quad \|S(m,n)P_n^u\| \leq K e^{-\alpha(n-m)}.$$

The corresponding **data** are $(K, \alpha, P_n^{s,u})$.

For the discrete case we refer to [24, Definition 2.1] and for the continuous time system, see [5], [11, Definition 7.6.1], [23, Chapter 2].

The next lemma, cf. [24, Lemma 2.7] establishes uniqueness and estimates for the bounded solution of an inhomogeneous equation.

Lemma A.1 *Assume that the difference equation $u_{n+1} = A_n u_n$, $u_n \in \mathbb{R}^k$, $n \in \mathbb{Z}$ has an exponential dichotomy on $\mathbb{Z}$ with data $(K, \alpha, P_n^{s,u})$ and let $r_{\mathbb{Z}}$, be a bounded sequence in $\mathbb{R}^k$.*
Then the inhomogeneous difference equation

$$u_{n+1} = A_n u_n + r_n, \quad n \in \mathbb{Z}$$

has a unique bounded solution $u_{\mathbb{Z}}$. Moreover the following estimate holds true for all $n \in \mathbb{Z}$

$$\|u_n\| \leq K(1 + e^{-\alpha})(1 - e^{-\alpha})^{-1} \|r_{\mathbb{Z}}\|_\infty .$$

Exponential dichotomies are robust under small additive perturbations of the equation.The Roughness–Theorem provides precise bounds on these perturbations, see [24, Proposition 2.10], [19, Lemma 2.3].

Theorem A.1 (Roughness–Theorem) *Assume that the difference equation $u_{n+1} = A_n u_n$ has an exponential dichotomy on $J = [n_-, n_+], n_\pm \in \mathbb{Z} \cup \{\pm\infty\}$ with data $(K, \alpha, P_n^{s,u})$.*

Then for $0 < \beta < \alpha$ and every $E_J \in (\mathbb{R}^{k,k})^J$ with

$$\|E_J\| \leq \frac{1}{2} \inf_{n \in J} \|A_n^{-1}\|^{-1}, \tag{A.1}$$

$$\|E_J\| \leq \frac{1}{2} K^{-1} \left(\frac{1}{e^\beta - e^{-\alpha}} + \frac{1}{e^{-\beta} - e^{-\alpha}} + \frac{1}{e^\alpha - e^{-\beta}} \right)^{-1}, \tag{A.2}$$

the equation

$$u_{n+1} = (A_n + E_n) u_n, \quad n \in J$$

has an exponential dichotomy on J with data $(2K + 1, \beta, Q_n^{s,u}(E_n))$.

A.2 A Lipschitz inverse mapping theorem

The following quantitative version of the Lipschitz inverse mapping theorem cf. [29, §3 Lemma 1], [18, Appendix C] is essential for proving Theorem 4.1.

Lemma A.2 *Let $F : Y \times \Lambda \to Z$ be a C^ℓ, $\ell \geq 1$ mapping from a Banach space $Y \times \Lambda$ into some Banach space Z. Assume there exists a function $\bar{v}_0 : \Lambda \to Y$ such that $F_v(\bar{v}_0(h), h)$ are homeomorphisms for all $|h| \leq \delta_2$, and there exist some constants $\kappa(h) > 0$, $\sigma(h) > 0$ such that for all $\|v - \bar{v}_0(h)\| \leq \delta_1$ and $|h| \leq \delta_2$ we have*

$$\|F_v(v,h) - F_v(\bar{v}_0(h),h)\| \leq \kappa(h) < \sigma(h) \leq \left\|F_v(\bar{v}_0(h),h)^{-1}\right\|^{-1}, \tag{A.3}$$

$$\|F(\bar{v}_0(h),h)\| \leq (\sigma(h) - \kappa(h))\delta_1. \tag{A.4}$$

Then for any $|h| \leq \delta_2$, $F(\cdot,h)$ has a unique zero $\tilde{v}(h)$ with $\|\tilde{v}(h) - \bar{v}_0(h)\| \leq \delta_1$ that is C^ℓ-smooth w.r.t. h. The following estimates hold for all $\|v_i - \bar{v}_0(h)\| \leq \delta_1,\ i = 1,2$

$$\|\tilde{v}(h) - \bar{v}_0(h)\| \leq (\sigma(h) - \kappa(h))^{-1} \|F(\bar{v}_0(h),h)\|,$$

$$\|v_1 - v_2\| \leq (\sigma(h) - \kappa(h))^{-1} \|F(v_1,h) - F(v_2,h)\|.$$

Acknowledgement

The authors thank an anonymous referee for constructive and helpful remarks, which improved the first version of this paper.

References

1. B. Aulbach. The fundamental existence theorem on invariant fiber bundles. *J. Differ. Equations Appl.*, 3(5-6):501–537, 1998.
2. W.-J. Beyn. The numerical computation of connecting orbits in dynamical systems. *IMA J. Numer. Anal.*, 10(3):379–405, 1990.
3. W.-J. Beyn, A. Champneys, E. Doedel, W. Govaerts, Y. Kuznetsov, and B. Sandstede. Chapter 4 numerical continuation, and computation of normal forms. Vol. 2 of *Handbook of Dynamical Systems*, pages 149 – 219. Elsevier Science, 2002.
4. W.-J. Beyn and J.-M. Kleinkauf. The numerical computation of homoclinic orbits for maps, *SIAM J. Numer. Anal.*, **34**, 1207–1236, 1997.
5. W. Coppel. *Dichotomies in stability theory.* Lecture Notes in Mathematics, vol. 629. Springer-Verlag, Berlin-New York, 1978.
6. J. England, B. Krauskopf, and H. Osinga. Computing one-dimensional stable manifolds and stable sets of planar maps without the inverse. *SIAM Journal on Applied Dynamical Systems*, 3(2):161–190, 2004.
7. B. Fiedler and J. Scheurle. Discretization of homoclinic orbits, rapid forcing and "invisible" chaos. *Mem. Amer. Math. Soc.*, 119(570):viii+79, 1996.
8. M. Friedman and E. Doedel. Computational methods for global analysis of homoclinic and heteroclinic orbits: A case study. *Journal of Dynamics and Differential Equations*, 5(1):37–57, 1993.
9. B. Garay. On C^j-closeness between the solution flow and its numerical approximation. *J. Differ. Equations Appl.*, 2(1):67–86, 1996.
10. J. Guckenheimer and P. Holmes. *Nonlinear oscillations, dynamical systems, and bifurcations of vector fields*, vol. 42. New York Springer Verlag, 1983.
11. D. Henry. *Geometric theory of semilinear parabolic equations*, vol. 840 of *Lecture Notes in Mathematics*. Springer-Verlag, Berlin-New York, 1981.
12. M. Hirsch, C. Pugh, and M. Shub. *Invariant Manifolds.* Number Nr. 583 in Lecture Notes in Mathematics. Springer-Verlag, 1977.

13. T. Hüls. Homoclinic orbits of non-autonomous maps and their approximation. *J. Difference Equ. Appl.*, 12(11):1103–1126, 2006.
14. T. Hüls. Numerical computation of dichotomy rates and projectors in discrete time. *Discrete Contin. Dyn. Syst. Ser. B*, 12(1):109–131, 2009.
15. T. Hüls. Computing Sacker-Sell spectra in discrete time dynamical systems. *SIAM J. Numer. Anal.*, 48(6):2043–2064, 2010.
16. T. Hüls. Homoclinic trajectories of non-autonomous maps. *Journal of Difference Equations and Applications*, 17(1):9–31, 2011.
17. T. Hüls. A contour algorithm for computing stable fiber bundles of nonautonomous, noninvertible maps. *Bielefeld University, CRC 701*, Preprint 14060, 2014.
18. M. Irwin. *Smooth dynamical systems*, vol. 17 of *Advanced Series in Nonlinear Dynamics*. World Scientific Publishing Co., Inc., River Edge, NJ, 2001. Reprint of the 1980 original, With a foreword by R. S. MacKay.
19. J.-M. Kleinkauf. The numerical computation and geometrical analysis of heteroclinic tangencies. Technical Report 98-052, Bielefeld University, SFB 343, 1998. http://www.math.uni-bielefeld.de/sfb343/preprints/index98.html.
20. B. Krauskopf and H. Osinga. Growing 1D and quasi-2D unstable manifolds of maps. *J. Comput. Phys.*, 146(1):404–419, 1998.
21. J. Langa, J. Robinson, and A. Suárez. Stability, instability, and bifurcation phenomena in non-autonomous differential equations. *Nonlinearity*, 15(3):887–903, 2002.
22. L. Lerman and L. Shil′nikov. Homoclinical structures in nonautonomous systems: nonautonomous chaos. *Chaos*, 2(3):447–454, 1992.
23. K. Palmer. Exponential dichotomies and transversal homoclinic points. *J. Differential Equations*, 55(2):225–256, 1984.
24. K. Palmer. Exponential dichotomies, the shadowing lemma and transversal homoclinic points. In *Dynamics reported*, vol. 1 of *Dynam. Report. Ser. Dynam. Systems Appl.*, pages 265–306. Wiley, Chichester, 1988.
25. C. Pötzsche and M. Rasmussen. Taylor approximation of integral manifolds. *Journal of Dynamics and Differential Equations*, 18(2):427–460, 2006.
26. M. Scheffer, S. Rinaldi, Y. Kuznetsov, and E. van Nes. Seasonal dynamics of daphnia and algae explained as a periodically forced predator-prey system. *Oikos*, 80:519–532, 1997.
27. L. Šil'nikov. Existence of a countable set of periodic motions in a neighborhood of a homoclinic curve. *Dokl. Akad. Nauk SSSR*, 172:298–301, 1967. Soviet Math. Dokl. 8 (1967), 102–106.
28. S. Smale. Differentiable dynamical systems. *Bulletin of the American mathematical Society*, 73(6):747–817, 1967.
29. G. Vainikko. Approximative methods for nonlinear equations (two approaches to the convergence problem). *Nonlinear Analysis, Theory. Methods and Applications.*, 2(6):647–687, 1978.
30. Y.-K. Zou and W.-J. Beyn. On manifolds of connecting orbits in discretizations of dynamical systems. *Nonlinear Analysis: Theory, Methods and Applications*, 52(5):1499 – 1520, 2003.